Generation and Compression of Chirped Biphotons

S. Sensarn,* G. Y. Yin, and S. E. Harris

Edward L. Ginzton Laboratory, Stanford University, Stanford, California 94305, USA

(Received 7 April 2010; revised manuscript received 3 June 2010; published 22 June 2010)

We describe an experiment demonstrating the radarlike technique of "chirp and compress." Chirped biphotons are generated using a quasi-phase-matched nonlinear crystal where the phase-matched frequency varies linearly with position. Sum frequency generation is used to measure the amplitude of the biphoton wave function. As compared to a nonchirped crystal, compression and an increase in summing efficiency of a factor of 5 is observed.

DOI: 10.1103/PhysRevLett.104.253602 PACS numbers: 42.50.Dv, 42.50.Ct, 42.65.Re

Entangled photon pairs, or biphotons, generated by spontaneous parametric down-conversion have the unique property that their energies and arrival times at distant detectors are linked [1]. With a monochromatic pump, the generated signal and idler photon energies are perfectly anticorrelated, and nonlinear processes such as two-photon absorption and sum frequency generation (SFG) may be highly resonant, e.g., with an atomic transition [2,3] or an optical cavity mode [4]. Temporal correlation between the photons is strongest when the bandwidths of the signal and idler are large. When the relative phase of the biphoton is properly corrected, the shortest possible correlation time is a single optical cycle [5]. As it bears on either sum frequency generation or two-photon absorption, a single-cycle biphoton will have an effective peak power of approximately $\frac{1}{2\pi}\hbar\omega_p^2$.

Ultrashort biphotons may be generated using chirped quasi-phase-matched (QPM) nonlinear crystals, which allow engineering of the phase-matching conditions, and therefore the frequencies and bandwidths of the photons, simply by varying the local poling period along the length of the crystal [6]. Because the biphotons are born with a chirp, subsequent compression is necessary to achieve the shortest possible correlation width. As a result of the quantum mechanical effect now termed as nonlocal dispersion compensation [7,8], this compression is additive and may be performed on either or both of the photons of the biphoton pair.

The amplitude of the biphoton wave packet may then be measured using SFG as an ultrafast correlator [9,10]. The chirp and compress technique, outlined in Fig. 1, allows short biphotons to be generated at a high emission rate using long crystals. In this Letter, we report the generation of chirped biphotons compressed to a correlation width of 130 fs, as compared to 0.7 ps for a nonchirped QPM crystal of the same length.

We note the recent work by Nasr and colleagues who have demonstrated Hong-Ou-Mandel interference using broadband biphotons generated with chirped QPM crystals. However, the short correlation time is the result of immunity to even-order terms in the relative phase and is not a measure of the actual width of the biphoton wave packet, which remains broad [11]. Recently, Brida *et al.* [12] have suggested the use of optical fiber as a practical implementation of the compression proposed in Ref. [5]. We follow their work, using bulk SF6 glass to compress the biphoton.

Our experimental setup is shown in Fig. 2. A 20-mm-long magnesium-oxide-doped stoichiometric lithium tantalate crystal (SLT, HC Photonics Corp.) is pumped by a confocally-focused 532-nm cw laser (Coherent Verdi V10). The biphotons are generated collinearly with the pump beam, and all fields are polarized along the extraordinary axis of the nonlinear crystal. In order to allow comparison between chirped or compressed and nonchirped biphotons, the generating crystal contains two QPM gratings. In the first, the spatial frequency of the domain reversals varies linearly from the input to the output end. In the second, the grating periodicity is independent of position. We switch between the two gratings by translating the crystal. The pump powers used are 7 and 6 W for the chirped and periodic gratings, respectively, and are limited by thermal lensing. The room-temperature (298 K) poling period varies from 8.0223 to 8.0481 μm for the chirped grating, while the period for the nonchirped grating is 8.0008 μm. The crystal is temperature tuned to generate signal photons with a center wavelength of 1000 nm as measured by a CCD spectrograph (Jarrell

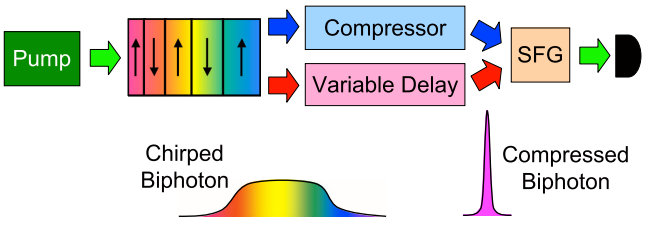

FIG. 1 (color online). Overview of "chirp and compress." Biphotons are generated by a chirped QPM crystal. The signal photon passes through a compressor and the idler through a variable delay. The photons are recombined in a summing crystal which serves as an ultrafast correlator.

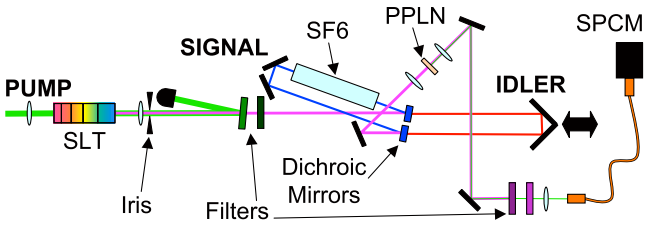

FIG. 2 (color online). Schematic of chirp and compress experiment. Biphotons are generated collinearly, filtered from the cw pump laser, and separated with dichroic mirrors. The signal photon is dispersed by an SF6 glass block, while the idler channel has a variable delay. The photons are recombined and focused into a PPLN crystal which generates a monochromatic beam of sum frequency photons.

Ash MonoSpec 27 with a single-mode fiber coupled to the input slit). The corresponding idler photons are centered at 1137 nm. The spectra for the chirped and nonchirped signal photons are shown in Fig. 3, with phase-matching temperatures of 301 and 320 K, respectively. The generated photon bandwidths are about 250 cm^{-1} for the chirped grating and 50 cm^{-1} for the nonchirped grating.

After a collimating lens, the biphoton and pump beams are apertured using an adjustable iris set to 2.5-mm diameter. The strong pump beam is removed from the weak biphotons using a pair of filters (Semrock LP02-568RS-25 and Schott RG695). After filtering, the biphoton flux measured by a silicon power meter is about 30 nW. Since silicon has a much lower quantum efficiency at the idler wavelength (1137 nm) than at the signal wavelength (1000 nm), almost all of the measured power corresponds to signal photons. This implies a pair-generation rate of about 1.5×10^{11} pairs/s.

The biphotons next enter a correlator which separates the signal from the idler. A dichroic mirror (Semrock LP02-1064RS-25) reflects the signal and transmits the idler photons. A 10-degree angle of incidence is chosen to shift the transmission edge of the mirror to the degenerate frequency of 1064 nm. The signal photon propagates through a fixed path containing a removable 80-mm-long block of dispersive SF6 glass that is used to compress the biphoton. The idler photon passes through a delay arm

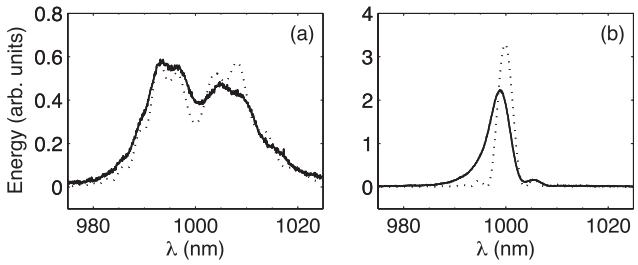

FIG. 3. Measured spectrum of the signal photon as generated by (a) chirped and (b) nonchirped QPM gratings in a 20-mm-long SLT crystal. Dotted curves are theoretical fits (see text).

which can be electronically scanned using an automated stage. The photons are recombined using a second dichroic mirror and focused into a 1-mm-long, periodically-poled, magnesium-oxide-doped lithium niobate crystal for SFG (PPLN, Thorlabs SHG3-1). The PPLN crystal is heated to 433 K for phase matching and has a calculated acceptance bandwidth of 1100 cm^{-1}. Generated 532-nm SFG photons are separated from the biphotons using filters (Schott BG39 and Semrock LL01-532-12.5) and coupled through multimode fiber to a single-photon counting module (SPCM, PerkinElmer SPCM-AQR-16-FC). The SFG count rate, expressed as a function of delay in the idler channel, is proportional to the second-order Glauber intensity correlation function or, equivalently, to the square of the amplitude of the biphoton wave packet [5]. The measured signal transmission from the input of the correlator to the output of the multimode fiber is 44%.

To demonstrate chirp and compress, we first orient the SLT crystal with the 8.0223-μm poling period on the input edge. Figures 4(a) and 4(b) show the measured SFG count rate as a function of the idler delay, without and with the SF6 glass block in the signal channel. The retroreflector in the idler channel is translated in 3-μm steps, delaying the idler by 20 fs/step. At each reflector position, 5-sec measurements of count rate are repeated 12 times and averaged for a single data point. Each error bar shows the standard deviation of the 12 measurements divided by $\sqrt{12}$. The correlation width in Fig. 4(b) is 130 fs (equal to the inverse of the 250-cm^{-1} photon bandwidth).

In contrast to the above orientation, we also measure the biphoton correlation with the QPM grating reversed

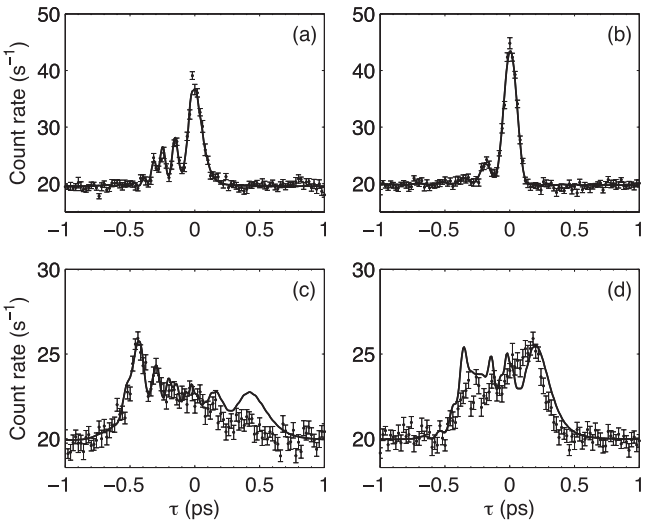

FIG. 4. Biphoton correlation measurements. SFG count rate as a function of idler delay, for the chirped SLT crystal oriented with the 8.0223-μm poling period on the input edge, is shown (a) without and (b) with an 80-mm-long SF6 glass block in the signal channel. Correlations (c) and (d) correspond to the reverse crystal orientation and the nonchirped grating, respectively. Curves are theoretical fits (see text).

(8.0481-μm period at the input edge) and by using the nonchirped grating (8.0008-μm period). Figures 4(c) and 4(d) show the resulting correlation data. Because of the reduced count rate in these correlations, 24 samples are used for each data point with error bars depicting standard deviations divided by $\sqrt{24}$. The nonchirped biphoton in Fig. 4(d) has a width of about 0.7 ps.

Comparing Figs. 4(b) and 4(d), using a chirped nonlinear crystal and subsequent compression reduces the biphoton correlation width, and increases the peak power of the biphoton, by a factor of 5.

In the down-conversion process, photons born at the output edge of the crystal experience no dispersion and arrive at distant detectors at the same time. In contrast, photons born at the input edge have a relative group velocity of $1/V_r = 1/V_s - 1/V_i$ and experience a relative group delay given by $\tau_D = L/V_r$ [13]. For a material with positive group velocity dispersion (GVD) such as SLT, the idler photon leads the signal photon by τ_D. Because the photons can be born anywhere inside the crystal, the relative delay for any given photon pair lies between 0 and τ_D, thereby giving rise to the wave packet width. To compress the wave packet, the bandwidth $\Delta\omega$ of the chirped biphotons must be large as compared to $2\pi/\tau_D$, and the maximum ratio of the compressed to the uncompressed correlation width is approximately $\frac{1}{2\pi}\tau_D\Delta\omega$.

When either or both of the photons enters a dispersive medium with positive GVD, compression may be achieved only with a particular orientation of the generating crystal. If the photons that are phase matched at the output edge of the chirped crystal have a larger wavelength difference than those at the input edge, these photons will be more strongly dispersed by the medium. After an optimal propagation length, the output-edge photons exit the medium with the same relative delay as the input-edge photons, and the wave packet width is therefore minimized. In our experiment, orienting our crystal with the 8.0223-μm poling period at the input edge satisfies the requirement for compression with positive GVD. In the opposite orientation, a dispersive medium must have negative GVD to compress the biphoton.

The solid curves in Figs. 4 are theoretical fits to the data. To produce these curves, we follow the theory of Harris describing biphoton generation with a chirped QPM crystal [5]. (We note that another, somewhat different approach to the theory of SFG with down-converted photons is described by Dayan [14].) We take the spatial frequency of the domain reversals to vary linearly with crystal length as $K_0 - \zeta z$, where K_0 is chosen to phase match a particular pair of signal and idler frequencies at the input end of the crystal. The parameter ζ defines the amount of chirp in the crystal and, in this experiment, is $|\zeta| = 1.26 \times 10^5\ \mathrm{m}^{-2}$. Both signal and idler frequencies are positive, and the signal frequency $\omega_s = \omega$ is defined to be in the range $\omega_p/2 \le \omega < \omega_p$. For a monochromatic pump at frequency ω_p, and with $\omega_i = \omega_p - \omega$, the signal and idler annihilation operators at the output of a crystal of length L are [5]

$$\begin{aligned} a_s(\omega, L) &= A_1(\omega)a_s(\omega, 0) + B_1(\omega)a_i^\dagger(\omega_i, 0), \\ a_i^\dagger(\omega_i, L) &= C_1(\omega)a_s(\omega, 0) + D_1(\omega)a_i^\dagger(\omega_i, 0), \end{aligned} \tag{1}$$

where $A_1(\omega) = \exp[ik_s(\omega)L]$, $D_1(\omega) = \exp[-ik_i(\omega_i)L]$, $C_1(\omega) = B_1^*(\omega)\exp[i(k_s(\omega) - k_i(\omega_i))L]$, and

$$\begin{aligned} B_1(\omega) = -(-1)^{1/4}\left(\frac{\pi}{2\zeta}\right)^{1/2}\kappa\exp[ik_s(\omega)L] \\ \times \exp\left[\frac{-i\Delta k(\omega)^2}{2\zeta}\right]\left\{\mathrm{erfi}\left[\frac{(1+i)\Delta k(\omega)}{2\sqrt{\zeta}}\right]\right. \\ \left. - \mathrm{erfi}\left[\frac{(1+i)(\Delta k(\omega) + \zeta L)}{2\sqrt{\zeta}}\right]\right\}. \end{aligned} \tag{2}$$

In Eq. (2), κ is a constant proportional to the pump electric field, $\Delta k(\omega) = k_p(\omega_p) - [k_s(\omega) + k_i(\omega_i) + K_0]$, and erfi is the imaginary error function. In general, $k_j(\omega) = n_j(\omega)\omega/c$; in our experiment, all fields are polarized along the same axis of the nonlinear crystal and see the same refractive index $n(\omega)$. Time- and frequency-domain field operators are related by Fourier transform: $a(t, z) = \int_{-\infty}^{\infty} a(\omega, z)\exp(-i\omega t)d\omega$.

The power spectral density of the signal photon, which also defines that of the idler photon by energy conservation, is [5]

$$S(\omega) = \frac{1}{2\pi}|B_1(\omega)|^2, \tag{3}$$

with the total pair-generation rate given by $R = \int_{\omega_p/2}^{\omega_p} S(\omega)d\omega$. The dotted curves in Fig. 3 are calculated using Eq. (3) with the Sellmeier equation for SLT [15]. They are both scaled by the same factor to best fit Fig. 3(a). [The phase-matching temperatures used to calculate the curves in Figs. 3(a) and 3(b) are 311 and 328 K, respectively.]

Equations (1) describe the photons at the exit face of the crystal; to propagate the fields through arbitrary optical systems and model the correlation measurement, $a_s(\omega, L)$ and $a_i(\omega_i, L)$ may be multiplied by transfer functions $H(\omega)$ and $G(\omega_i, \tau)$, respectively, where τ represents the variable delay in the idler channel. The coefficients in Eqs. (1) become new coefficients $A(\omega) = H(\omega)A_1(\omega)$, $B(\omega) = H(\omega)B_1(\omega)$, $C(\omega, \tau) = G^*(\omega_i, \tau)C_1(\omega)$, and $D(\omega, \tau) = G^*(\omega_i, \tau)D_1(\omega)$.

When the signal and idler photons are recombined and focused into a thin nonlinear crystal for correlation, the SFG photon rate is [5]

$$R_{\mathrm{sum}}(\tau) = \eta_1\left[R^2 + \left|\left(\frac{1}{2\pi}\right)\int_{\omega_p/2}^{\omega_p} A(\omega)C^*(\omega, \tau)d\omega\right|^2\right], \tag{4}$$

where the constant η_1 includes such factors as loss in the optical system, nonlinearity, length, and poling quality of the summing crystal, spatial-mode matching, and detection efficiency. The first term in Eq. (4) represents broadband SFG photons produced by the classical summing of uncorrelated photons from different pairs. For a monochromatic pump, the second term is monochromatic and arises from SFG between entangled photons [5]. Dropping the first term and denoting $\psi(\omega) = \frac{1}{2\pi} A_1(\omega) C_1^*(\omega)$, Eq. (4) becomes

$$R_{\mathrm{sum}}(\tau) = \eta_1 \left| \int_{\omega_p/2}^{\omega_p} H(\omega) G(\omega_i, \tau) \psi(\omega) d\omega \right|^2. \quad (5)$$

We assume that all of the dispersion caused by filters, mirrors, and lenses in the system is limited to second order (GVD). Because GVD acting on the signal or idler is additive in its effect on the biphoton [7], we lump all such dispersive elements into $H(\omega)$ as a single, equivalent GVD term. $H(\omega)$, which also includes the dispersion of the removable SF6 glass block in the signal channel, is therefore defined as

$$H(\omega) = \exp\left[i \frac{\beta}{2} (\omega - \omega_0)^2 + i k_g(\omega) L_g \right], \quad (6)$$

where β is a constant representing the GVD of the optical system, ω_0 is the center frequency of the signal, and the $k_g(\omega) = n_{\mathrm{SF6}}(\omega)\omega/c$ is the wave vector for the signal photon in the SF6 glass block of length L_g. For the case where the glass block is present in the signal channel, Fig. 4(b), we take $L_g = 80$ mm; otherwise, $L_g = 0$. Although all orders of dispersion are included using the Sellmeier equation for SF6 glass, the GVD term is dominant with a value of 143 $\mathrm{fs}^2/\mathrm{mm}$ at the 1000-nm signal wavelength. The 80-mm glass length approximately satisfies the estimate required for compression given in Ref. [5]: $H(\omega) \sim \exp[i\tau_D(\omega - \omega_0)^2/(2\Delta\omega)]$.

The solid curves in Figs. 4 are plots of Eq. (5) with $G(\omega_i, \tau) = \exp(i\omega_i\tau)$. Figures 4(a) and 4(b) use $\zeta = 1.26 \times 10^5\ \mathrm{m}^{-2}$, while Fig. 4(c) uses $\zeta = -1.26 \times 10^5\ \mathrm{m}^{-2}$. Figure 4(d) uses $\zeta = 10^{-6}\ \mathrm{m}^{-2}$ to approximate the nonchirped grating. The scale factor $\eta_1\kappa^2$ and the dispersion constant β are used as fitting parameters and are chosen to minimize mean-square error for the data in Figs. 4(a)–4(c), which correspond to large-bandwidth biphotons that depend strongly on dispersion. Each theory curve is independently time shifted for best fit with the data and vertically shifted by the dark-count level. The optimal values for the fitting parameters are $\eta_1\kappa^2 = 7.83 \times 10^{-21}\ \mathrm{s/m}^2$ and $\beta = 3600\ \mathrm{fs}^2$.

In summary, this work reports a first experimental demonstration of the chirp and compress technique for generating short biphotons. We achieve a compressed biphoton correlation width of 130 fs, a factor of 5 shorter than a periodically poled crystal source of the same length. The efficiency of sum frequency generation increases by this same factor, indicating an increase in the effective peak power of the biphoton. Calculation, as outlined in the previous text, shows that this is the maximum compression that is obtainable using our lithium tantalate crystal, pump wavelength, and a linear chirp. Further improvements to the correlation width and peak power of the biphoton will require third- and higher-order dispersion control [16,17]. [The small side-lobe in Fig. 4(b) indicates the onset of third-order dispersion that must be compensated if larger chirps are used.] Instead, it is probable that the chirping profile itself may be designed to precompensate for higher-order dispersion further along in the optical system.

The authors thank Marty Fejer for helpful discussions. This work was supported by the U.S. Air Force Office of Scientific Research and the U.S. Army Research Office.

*sensarn@stanford.edu

[1] Y. Shih, Rep. Prog. Phys. **66**, 1009 (2003).
[2] B. Dayan, A. Pe'er, A. A. Friesem, and Y. Silberberg, Phys. Rev. Lett. **93**, 023005 (2004).
[3] H. You, S. M. Hendrickson, and J. D. Franson, Phys. Rev. A **80**, 043823 (2009).
[4] S. Sensarn, I. Ali-Khan, G. Y. Yin, and S. E. Harris, Phys. Rev. Lett. **102**, 053602 (2009).
[5] S. E. Harris, Phys. Rev. Lett. **98**, 063602 (2007).
[6] A. F. Abouraddy, M. B. Nasr, B. E. A. Saleh, A. V. Sergienko, and M. C. Teich, Phys. Rev. A **65**, 053817 (2002).
[7] J. D. Franson, Phys. Rev. A **45**, 3126 (1992).
[8] S. Y. Baek, Y. W. Cho, and Y. H. Kim, Opt. Express **17**, 19 241 (2009).
[9] A. Pe'er, B. Dayan, A. A. Friesem, and Y. Silberberg, Phys. Rev. Lett. **94**, 073601 (2005).
[10] K. A. O'Donnell and A. B. U'Ren, Phys. Rev. Lett. **103**, 123602 (2009).
[11] M. B. Nasr *et al.*, Phys. Rev. Lett. **100**, 183601 (2008).
[12] G. Brida *et al.*, Phys. Rev. Lett. **103**, 193602 (2009).
[13] M. H. Rubin, D. N. Klyshko, Y. H. Shih, and A. V. Sergienko, Phys. Rev. A **50**, 5122 (1994).
[14] B. Dayan, Phys. Rev. A **76**, 043813 (2007).
[15] A. Bruner *et al.*, Opt. Lett. **28**, 194 (2003).
[16] R. L. Fork, C. H. B. Cruz, P. C. Becker, and C. V. Shank, Opt. Lett. **12**, 483 (1987).
[17] A. M. Weiner, Rev. Sci. Instrum. **71**, 1929 (2000).